Journal of Environmental Radioactivity 120 (2013) 94–103

Contents lists available at SciVerse ScienceDirect

Journal of Environmental Radioactivity

journal homepage: www.elsevier.com/locate/jenvrad

Short-term variability of ^{7}Be atmospheric deposition and watershed response in a Pacific coastal stream, Monterey Bay, California, USA

Christopher H. Conaway [a,b,*], Curt D. Storlazzi [a], Amy E. Draut [a], Peter W. Swarzenski [a]

[a] U.S. Geological Survey, 400 Natural Bridges Drive, Santa Cruz, CA 95060, USA
[b] Institute of Marine Sciences, University of California, 1156 High Street, Santa Cruz, CA 95064, USA

ARTICLE INFO

Article history:
Received 17 October 2012
Received in revised form
30 January 2013
Accepted 7 February 2013
Available online 6 March 2013

Keywords:
^{7}Be atmospheric deposition
Rainwater
Central California
River water
Small mountainous rivers
Watersheds

ABSTRACT

Beryllium-7 is a powerful and commonly used tracer for environmental processes such as watershed sediment provenance, soil erosion, fluvial and nearshore sediment cycling, and atmospheric fallout. However, few studies have quantified temporal or spatial variability of ^{7}Be accumulation from atmospheric fallout, and parameters that would better define the uses and limitations of this geochemical tracer. We investigated the abundance and variability of ^{7}Be in atmospheric deposition in both rain events and dry periods, and in stream surface-water samples collected over a ten-month interval at sites near northern Monterey Bay (37°N, 122°W) on the central California coast, a region characterized by a rainy winters, dry summers, and small mountainous streams with flashy hydrology. The range of ^{7}Be activity in rainwater samples from the main sampling site was 1.3–4.4 Bq L^{-1}, with a mean (±standard deviation) of 2.2 ± 0.9 Bq L^{-1}, and a volume-weighted average of 2.0 Bq L^{-1}. The range of wet atmospheric deposition was 18–188 Bq m^{-2} per rain event, with a mean of 72 ± 53 Bq m^{-2}. Dry deposition fluxes of ^{7}Be ranged from less than 0.01 up to 0.45 Bq m^{-2} d^{-1}, with an estimated dry season deposition of 7 Bq m^{-2} month^{-1}. Annualized ^{7}Be atmospheric deposition was approximately 1900 Bq m^{-2} yr^{-1}, with most deposition via rainwater (>95%) and little via dry deposition. Overall, these activities and deposition fluxes are similar to values found in other coastal locations with comparable latitude and Mediterranean-type climate. Particulate ^{7}Be values in the surface water of the San Lorenzo River in Santa Cruz, California, ranged from <0.01 Bq g^{-1} to 0.6 Bq g^{-1}, with a median activity of 0.26 Bq g^{-1}. A large storm event in January 2010 characterized by prolonged flooding resulted in the entrainment of ^{7}Be-depleted sediment, presumably from substantial erosion in the watershed. There were too few particulate ^{7}Be data over the storm to accurately model a ^{7}Be load, but the results suggest enhanced watershed export of ^{7}Be from small, mountainous river systems compared to other watershed types.

Published by Elsevier Ltd.

1. Introduction

Owing to its short half-life ($T_{1/2}$ = 53.3 d), its well-known atmospheric production rate, and its relative simplicity in measurement using high-resolution γ-ray (gamma-ray) spectrometry, ^{7}Be is a powerful tracer for a diverse suite of environmental processes, including atmospheric mixing and fallout (Turekian et al., 1983; Baskaran et al., 1993; Graham et al., 2003; Baskaran and Swarzenski, 2007; Kaste and Baskaran, 2011). As such, ^{7}Be is commonly used in many studies to quantify watershed sediment provenance (Olsen et al., 1985; Cooper et al., 1991; Blake et al., 1999); soil and sediment erosion rates (Wallbrink and Murray, 1996; Matisoff et al., 2002; Walling et al., 2009); fluvial, estuarine, and coastal sediment cycling (Sommerfield et al., 1999; Matisoff et al., 2005; Corbett et al., 2007; Jweda et al., 2008; Draut et al., 2009; Zhu and Olsen, 2009); and general atmospheric fallout processes (Baskaran, 1995; Graham et al., 2003; Ayub et al., 2009; Pham et al., 2011). However, many studies that utilize ^{7}Be as a sediment tracer in fluvial, estuarine, and coastal settings have not quantified temporal or spatial variability of its accumulation and discharge in watershed source areas, and thus the extent of ^{7}Be retention in watersheds under various hydrologic conditions deserves further study. In this study, we evaluated variability in ^{7}Be activity in atmospheric deposition and surface-water samples in one small watershed over a 10-month interval to better understand potential uses and limitations of this geochemical tracer.

Beryllium-7 is primarily produced continuously in the stratosphere by cosmic-ray spallation reactions involving oxygen and nitrogen (Arnold and Al-Salih, 1955; Yoshimori, 2005). The cosmic

* Corresponding author. Present address: U.S. Geological Survey, 345 Middlefield Road MS427, Menlo Park, CA 94025, USA. Tel.: +1 650 329 4516.
E-mail address: cconaway@usgs.gov (C.H. Conaway).

0265-931X/$ – see front matter Published by Elsevier Ltd.
http://dx.doi.org/10.1016/j.jenvrad.2013.02.004

rays primarily involved in ^{7}Be production can be deflected by both the Sun's heliosphere and Earth's magnetosphere, thus ^{7}Be production rates vary inversely with the magnetic field strengths of these features. (Koch et al., 1996; Vonmoos et al., 2006; Berggren et al., 2009). The amount of ^{7}Be that reaches the Earth's surface is dependent on its atmospheric production rate, stratosphere–troposphere air exchange, and tropospheric circulation (Husain et al., 1977; Baskaran, 1995; Ishikawa et al., 1995; Masarik and Beer, 2009), and as a result the flux of ^{7}Be from the atmosphere to Earth is latitude dependent. Generally, the deposition of ^{7}Be scales with rainfall, and in most areas ^{7}Be dry deposition is much less important than is wet deposition (Olsen et al., 1985; Wallbrink and Murray, 1994; Whiting et al., 2005; Zhu and Olsen, 2009). Once transferred from the atmosphere to the Earth's surface, ^{7}Be quickly adsorbs to above-ground vegetation and soil in terrestrial systems, and onto suspended particles in fluvial and marine systems (Olsen et al., 1986). In fresh and marine waters, the distribution coefficient (K_d) of ^{7}Be range is on the order of 10^4–10^6 (Hawley et al., 1986; Olsen et al., 1986; You et al., 1989; Kaste and Baskaran, 2011), indicating ^{7}Be affinity for particulate matter.

The San Lorenzo River (37°N, 122°W) has a 350 km^2 watershed reaching from the Santa Cruz Mountains to the northern part of Monterey Bay on the central California coast (Fig. 1). Much of the watershed is forested (redwood and mixed redwood forest), with some urban patches, such as the lower reach of the river in the City of Santa Cruz. The watershed is part of a tectonically active landscape with major modifications by activities such as intensive logging in the late 19th century and flood-control engineering in the 1950s for the City of Santa Cruz. This area has a Mediterranean-type climate with a rainy season that usually lasts from November to April; the greatest volume of rainfall occurs during energetic winter storm events (Nuss, 1996). On average, there is little or no rainfall during the summer months. Fog in the area is common, especially in the summer months, as a result of typical eastern Pacific stratus cloud coverage and local, shallow cyclonic circulation (Archer et al., 2005). Intense winter storms often produce high-intensity rain and flashy, highly variable hydrology in the San Lorenzo River – a single storm event in the river basin can yield most of the annual water and sediment load over the course of a few days (Best and Griggs, 1991; Draut et al., 2011). The system is typical of many of the small, mountainous rivers on the California coast (Inman and Jenkins, 1999; Farnsworth and Milliman, 2003), and, globally, this type of watershed contributes substantial sediment loads to the marine environment (Milliman and Syvitski, 1992).

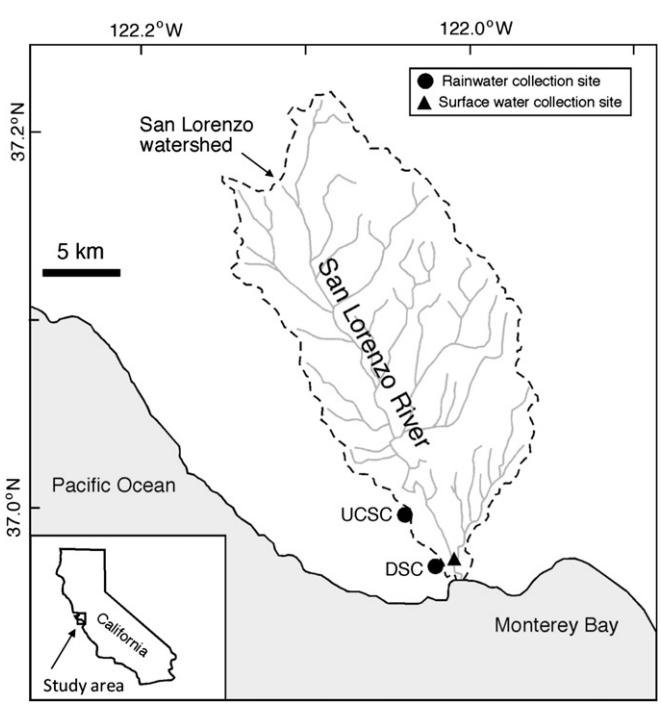

Fig. 1. Map illustrating the San Lorenzo River watershed on the northern part of Monterey Bay and collection sites for atmospheric deposition and surface-water samples.

Because the sediment load of the San Lorenzo River contains a substantial fine-grained fraction that can efficiently scavenge particle-reactive constituents, this river system is an efficient vector for delivering a diverse suite of sediment-hosted contaminants to the adjacent coastal ocean (Conaway et al., 2012). As a consequence, it is of interest to know where in the watershed the likely source regions for newly eroded sediment are located, what the transport time might be for a particle to travel downstream to the sea, what types of contaminants are attached to particle surfaces and so delivered to the coastal ocean, and how these contaminants are distributed in the nearshore environment. One technique that can provide some information on these processes involves examining the temporal variation in ^{7}Be activity in suspended sediment (Sommerfield et al., 1999; Matisoff et al., 2005). In addition, recent work has attempted to develop and refine models for using ^{7}Be to investigate soil redistribution by erosion (Walling et al., 1999, 2009). The success of such modeling efforts depends in part on an improved understanding of the temporal variation of ^{7}Be atmospheric deposition over the course of single and multiple rain events.

In this study, we report time-series measurements of ^{7}Be in atmospheric deposition samples collected over the course of 10 months during rain events and the intervening dry periods, and in surface-water samples collected in the lower reaches of the San Lorenzo River system. These data are discussed in terms of atmospheric deposition trends and applied to study watershed dynamics. This information provides a rare concurrent evaluation of variability in ^{7}Be atmospheric deposition and activity in fluvial suspended sediment within the same watershed and is used to improve understanding of the processes that control the fate of sediment-hosted contaminants.

2. Material and methods

Atmospheric deposition samples ($n = 42$) were collected during rain events and intervening dry periods between October 2009 and August 2010 at two locations in Santa Cruz County (Fig. 1). Surface-water samples were collected during rain events from one location in the lower reach of the San Lorenzo River, approximately 2 km upstream of the river mouth.

Daily rainfall and other weather data were collected from a weather station within the Santa Cruz region (PWS KCASANTA134 at 36.973°N, 122.040°W). Long-term (1898–2011) average monthly and yearly rainfall statistics were obtained for the National Climate Data Center station in Santa Cruz County (Station 047916 at 36.967°N, 122.017°W). Stream-flow data for the San Lorenzo River were obtained from the U.S. Geological Survey National Water Information System for the San Lorenzo River at Santa Cruz gaging station 11161000 (NWIS, 2012).

The main sampling site for atmospheric deposition was located on the roof of a 6-story building at the University of California at Santa Cruz (UCSC). Some additional samples were collected on top of a 3-m high platform in downtown Santa Cruz (DSC). Both rainwater and dry deposition samples were collected in 20-L high-density polyethylene containers with a 670 cm^2 opening. Collectors were pre-cleaned by rinsing three times with 500 mL 10% (v/v)

trace-metal grade HCl followed by a rinse with deionized water. Rainwater collectors were deployed on predicted days of rainfall with a pre-charge of 250 mL 10% (v/v) trace-metal grade HCl to prevent sorption of ^{7}Be to container surfaces. In addition, collectors were covered with an acid-cleaned 1.0 cm mesh plastic screen to prevent disturbance by and harm to animals. At the end of substantial rainfall, collectors were sealed and returned to the laboratory, with sample collection typically lasting 1–4 d. Total rainfall per event was measured using a standard rain gage, which gave nearly identical results (average 2% relative percent difference) to total rainfall calculated using the sample collectors ("bucket catch"). Sample collection for dry periods was performed using similar methods during times with no measurable rainfall, and collection times lasting about 5 d per sample.

Contents of the collectors were filtered (using 47-mm diameter, 0.45-μm pore size, cellulosic acetate material) to remove insects and other wind-blown particles using a HCl-cleaned glass vacuum filtration apparatus. The filtrate was transferred to a 4-L acid-cleaned glass beaker and brought to a total volume of 4 L by adding ultrapure (18 MΩ cm^{-1} resistivity) water. To this, 1.4 g of $FeCl_3$ were added and dissolved. The pH was then adjusted to basic (pH ~ 9) by adding KOH, causing the precipitation of iron oxyhydroxide with co-precipitation of ^{7}Be. The beaker with precipitate was then allowed to settle for 24 h and then the supernatant decanted. The remaining precipitate was rinsed with ultra-pure water into an acid-cleaned 300-mL jar and centrifuged (15 min at 3000 RPM), again with the supernatant being decanted. The remaining precipitate was then freeze dried, homogenized, and transferred to a 10 mL γ-ray counting vial and sealed.

Efficiency of ^{7}Be recovery in the method was estimated by spiking a subset of blanks and samples ($n = 6$) in the collectors with 1000 μg stable Be and measuring recovery in the iron oxyhydroxide precipitate. To determine the stable Be concentration, the precipitates were digested in 20 mL of concentrated HCl, and an analysis of a diluted aliquot of the digestate was made by inductively-coupled plasma mass spectrometry (ICP-MS) at the UCSC Institute of Marine Sciences. Mean spike recovery (±standard deviation) for stable Be was 94 ± 8%, with a range of 82–103%. This differs from the typical method of adding a stable Be carrier to every sample (Baskaran et al., 1993; Caillet et al., 2001; Kaste and Baskaran, 2011), however the ranges of recoveries for stable Be were deemed acceptable and no corrections were made to the ^{7}Be sample data based on stable Be recovery. Assuming that the stable carrier recovery was representative of the ^{7}Be recovery, this suggests ±8% uncertainty for the atmospheric deposition values. This uncertainty was apparently not reflected in the field replicates, as discussed below.

Concurrently with the time of rainwater sampling, unfiltered surface-water samples were collected from the San Lorenzo River by lowering an acid-cleaned 20-L bucket off of a bridge into the river, recovering about 15 L of water. The suspended sediment in water samples was allowed to settle for 3 d in the containers and then the overlying water was siphoned off to a remaining volume of 4 L. This volume was poured through a 0.425-mm screen to remove leaves and other large debris, and into a 4-L beaker and evaporated to dryness at 60 °C on a hot plate. The remaining sediment was weighed, homogenized with a mortar and pestle, and transferred to fill a 10 mL γ-ray counting vial and sealed. Because of the high affinity of ^{7}Be for particles in freshwater (Olsen et al., 1986; Kaste and Baskaran, 2011) and the relatively high suspended-sediment concentration in our surface-water samples (~100–1000 mg/L) compared to other systems, the unfiltered surface water values are reported as particulate ^{7}Be activity. Because substantial amounts of debris and large objects such as uprooted trees were being transported during storm-induced flooding, it was not practical to collect large volumes of depth-integrated sample from the river. Although measuring ^{7}Be activity in the surface-collected suspended sediment does not lead to a fully quantitative measure of ^{7}Be transported by the river, it allows for a comparison to variation in ^{7}Be atmospheric deposition and first approximation of watershed yield of ^{7}Be.

The ^{7}Be activity in samples was determined using an ultra-low background high-purity germanium (HPGe) well detector measuring 477.6 keV γ-ray emissions from the decay of ^{7}Be to ^{7}Li via electron capture. The HPGe detector is regularly calibrated using IAEA and NIST standards for a full range (1–10 mL) of geometries and like material, and the ^{7}Be detection efficiency is extrapolated from calibrations of these standards over the entire energy spectrum. Reported uncertainties reflect propagated errors arising from 1-σ counting error, the detector efficiency calibrations, and the background correction. Background activities of the detector are also monitored and accounted for regularly. The detector time per sample (count time) was typically about 1 d. The final ^{7}Be activities were decay corrected to the middle of their collection period. The average relative percent difference (±standard deviation) on duplicate samples from co-located collectors in the field was 4.1 ± 2.0% for ^{7}Be ($n = 3$), which indicates much better precision than the stable Be carrier results suggest for the ^{7}Be measurements. Procedural ^{7}Be blanks were less than 1% of the lowest sample for wet deposition (1.2 Bq), whereas some dry deposition samples were below the estimated minimum detectable amount, about 0.03 Bq on a sample counted for 1 d, which for the collector translates to about 0.6 Bq m^{-2} or 0.1 Bq m^{-2} d^{-1} for a typical 5-d collection period and about two weeks elapsed time between sampling and counting. Propagated ^{7}Be uncertainties were typically below 10%.

Rainfall events were examined using air-mass back-trajectory calculations generated using the HYSPLIT (HYbrid Single-Particle Lagrangian Integrated Trajectory) model (Draxler and Rolph, 2012; Rolph, 2012). Models used the website version and Global Data Assimilation System (GDAS1) dataset. Single trajectories were used with a starting point in Santa Cruz, CA (36.973°N, 122.040°W). Backward trajectory direction, Model Vertical Velocity vertical motion calculation, start times using the end of rainfall, a run time of 72 h, starting a new trajectory every 24 h back through the course of every day of the rain event, and a starting height of 500 m above ground level were used.

3. Results and discussion

3.1. Climate, weather, and hydrology during the sampling interval

The 10-month sampling interval, which began in October 2009 at the onset of the rainy season, was characterized by both exceptionally wet and dry months, as well as two notable storm events (Fig. 2A). The remnants of Typhoon Melor hit the central California coast in mid-October 2009, bringing heavy rainfall (381–508 mm in <24 h in parts of the Santa Cruz Mountains), high wind speeds (gusts >130 km h^{-1}), and local flooding (NOAA, 2009). The month of November 2009 was exceptionally dry (Fig. 2B), with total of 4.8 mm rainfall compared to 1898–2011 average November rainfall of 84.1 ± 70.6 mm (WRCC, 2012). In January 2010, a series of extra-tropical cyclones hit the west coast of the United States with heavy rainfall, hurricane force winds, and tornadoes, setting record low-pressures in California, Oregon, and Arizona (NOAA, 2010). The first in the series of January storms had the greatest impact on the central California coast. The peak discharge in the San Lorenzo River (Fig. 2C) occurred 20 January 2010 – a flood peak with an estimated 4–5 y return interval (Conaway et al., 2012). This storm event produced the majority of suspended sediment transport in the river for the year (Conaway et al., 2012). After the January

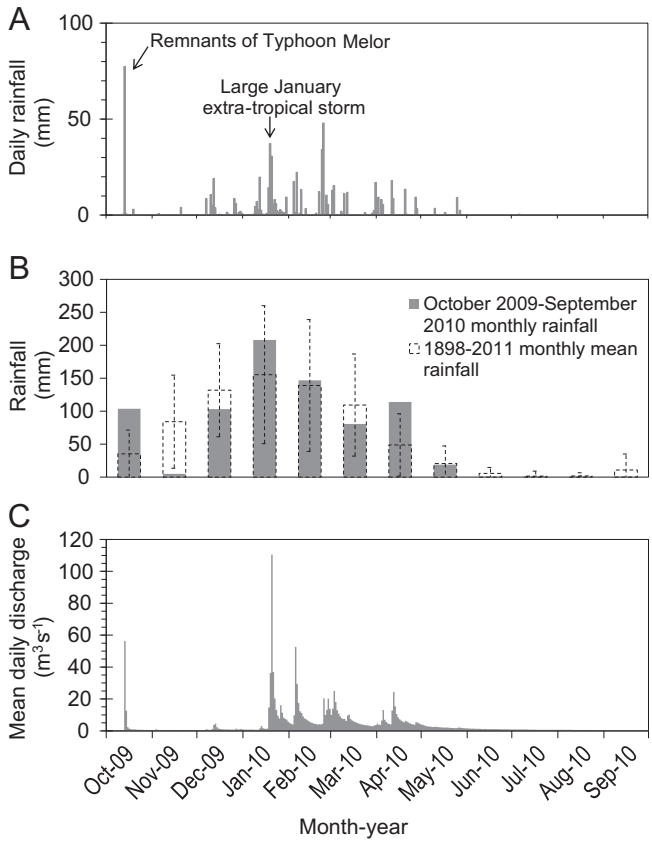

Fig. 2. Daily and monthly rainfall measured in Santa Cruz, California, and watershed response. A) Daily rainfall from October 2009–September 2010, with two notable storm events highlighted. B) Total monthly rainfall for the season compared to mean monthly values from a 114 y historic record (1898–2011). Error bars show ± one standard deviation for the historic means. C) Mean daily discharge in the San Lorenzo River.

storms, a few smaller storms occurred through the end of the rainy season and there was a relatively high April monthly rainfall compared to the historic record. The total precipitation for the year (781 mm) was close to the 1898–2011 average annual value of 763 ± 243 mm (WRCC, 2012).

3.2. Summary and statistics of ^{7}Be activity in atmospheric deposition

The activity of ^{7}Be in rainwater and ^{7}Be atmospheric deposition observed in the rain event collections (Table 1) are similar to those observed in other locations (Ayub et al., 2009; Kaste and Baskaran, 2011; Lozano et al., 2011). The ^{7}Be activities in rainwater samples ($n = 23$) from our main site (UCSC) ranged 1.3–4.4 Bq L^{-1}, with a mean (±standard deviation) of 2.2 ± 0.9 Bq L^{-1}, and a median of 2.1 Bq L^{-1}. The range is within that generally reported for ^{7}Be in rainwater, which is about 0.01–10 Bq L^{-1} (Ayub et al., 2009; Kaste and Baskaran, 2011), and also similar to the range 0.03–7.42 Bq L^{-1} and mean 2.5 Bq L^{-1} reported by Lozano et al. (2011) for the Mediterranean coast of Spain, which has a comparable latitude and climate to coastal California. The volume weighted average of the samples (2.0 Bq L^{-1}) falls in the range (about 1–2 Bq L^{-1}) compiled for precipitation-based collectors at various locations between latitudes 30–40°N by Kaste and Baskaran (2011). Measured wet deposition of ^{7}Be for the rain events at the main site ranged 18–188 Bq m^{-2}, with a mean of 72 ± 53 Bq m^{-2}, and a median of 63 Bq m^{-2}.

An examination of the relation between ^{7}Be activity, rainfall, and storm arrival direction shows mixed results, as indicated by a graphical analysis of ^{7}Be activity in rainwater (Bq L^{-1}) or ^{7}Be wet deposition (Bq m^{-2}) plotted against total rainfall (Fig. 3). Typically the greatest rainfall in the northern Monterey Bay area, which falls between December and March, is delivered by storms originating from the central Pacific that propagate into the study area from the southeast and southwest. The remnants of Typhoon Melor in October 2009, the January 2010 extra-tropical storms, and other storm systems arriving mostly from the south typically had high

Table 1
Beryllium-7 activity in rainwater samples (Bq L^{-1}) and wet deposition (Bq m^{-2}) from coastal sites in northern Monterey Bay. Uncertainties reflect propagated errors arising from 1σ counting error. Location of collection sites UCSC and DSC are shown on Fig. 1.

Site	Time interval (Month/day/year)	Rainfall (mm)	^{7}Be (Bq L^{-1})	^{7}Be (Bq m^{-2})	Storm arrival direction or storm information
UCSC	10/11/09–10/13/09	140	1.3 ± 0.0[a]	174 ± 4[a]	Typhoon Melor remnants
UCSC	11/19/09–11/20/09	7	2.5 ± 0.1	18 ± 1	North (along coast)
UCSC	12/06/09–12/07/09	10	2.2 ± 0.1	21 ± 1	North (along coast)
UCSC	12/10/09–12/13/09	62	2.1 ± 0.0[a]	134 ± 2[a]	South
UCSC	01/11/10–01/13/10	24	4.4 ± 0.1	98 ± 2	Extra-tropical cyclone
UCSC	01/16/10–01/18/10	55	2.1 ± 0.1	120 ± 3	Extra-tropical cyclone
UCSC	01/18/10–01/21/10	72	2.6 ± 0.0	188 ± 3	Extra-tropical cyclone
UCSC	01/21/10–01/22/10	25	2.9 ± 0.1	72 ± 2	Extra-tropical cyclone
UCSC	01/24/10–01/26/10	45	1.5 ± 0.0	71 ± 2	Extra-tropical cyclone
UCSC	02/01/10–02/05/10	45	1.8 ± 0.0	80 ± 2	Extra-tropical cyclone
UCSC	02/05/10–02/07/10	24	1.4 ± 0.0	31 ± 1	West and Northwest
UCSC	02/18/10–02/22/10	14	1.8 ± 0.1	26 ± 1	West and Northwest
UCSC	02/25/10–02/27/10	21	1.4 ± 0.1	30 ± 1	Mixed directions
DSC	02/25/10–02/27/10	17	1.4 ± 0.1	25 ± 1	Mixed directions
UCSC	03/02/10–03/05/10	24	2.1 ± 0.1	55 ± 1	Northwest
UCSC	04/02/10–04/03/10	34	1.3 ± 0.0	42 ± 1	Northwest
DSC	04/02/10–04/03/10	12	2.1 ± 0.1	27 ± 1	Northwest
UCSC	04/03/10–04/05/10	24	3.4 ± 0.2	77 ± 5	Northwest
DSC	04/03/10–04/05/10	15	2.0 ± 0.2	30 ± 2	Northwest
UCSC	04/10/10–04/12/10	38	3.5 ± 0.1	129 ± 5	North (along coast)
UCSC	04/18/10–04/21/10	13	2.0 ± 0.2	28 ± 3	Mixed directions
UCSC	04/26/10–04/27/10	22	1.4 ± 0.1[a]	32 ± 3[a]	West
DSC	04/26/10–04/27/10	12	2.0 ± 0.2	22 ± 2	West
UCSC	05/24/10–05/26/10	15	1.3 ± 0.1	18 ± 2	Northwest

[a] average of field replicates.

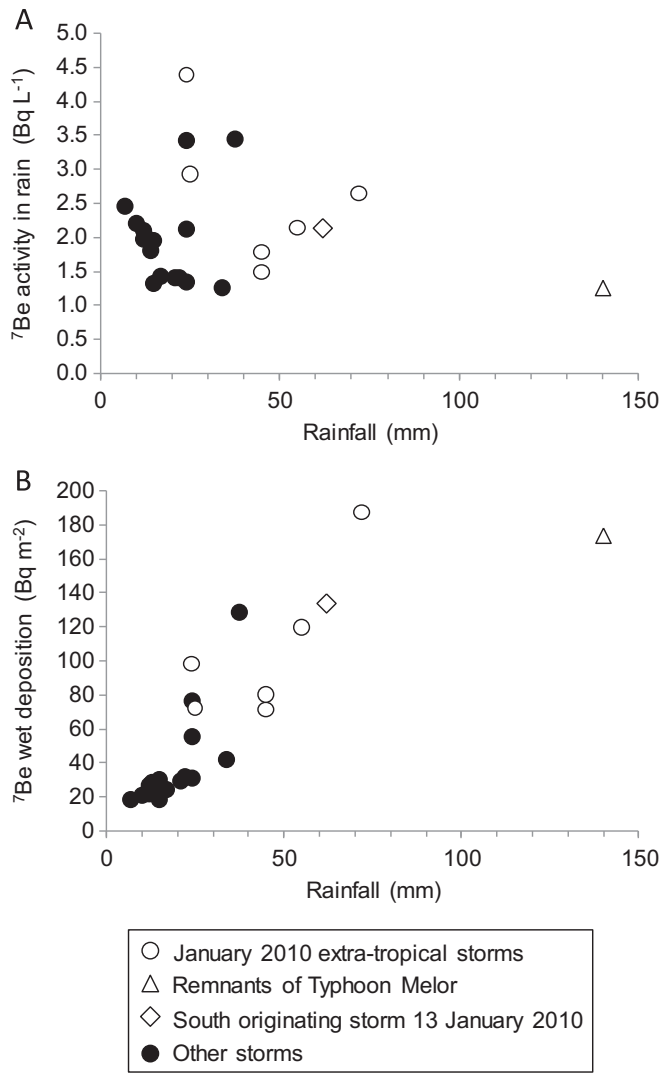

Fig. 3. ^{7}Be activity in rain event samples from the UCSC site. Data represent single and multiple samples from individual rain events. Duration of collection times are given on Table 1. A) ^{7}Be activity in rain versus rainfall. B) ^{7}Be wet deposition versus rainfall.

rainfall (20–140 mm), variable activity of ^{7}Be (Fig. 3A), and represented the highest deposition of ^{7}Be (Fig. 3B). Other storm events, arriving mostly from the north and northwest, delivered less rainfall (typically <40 mm). One feature of these other storms is that there tends to be less ^{7}Be activity with increasing rainfall (Fig. 3A), but more ^{7}Be deposition (Fig. 3B). These results suggest that ^{7}Be activity in rain is not predictable when considering only the origin of the rain storm, and that ^{7}Be wet deposition is mostly a function of total rainfall for a given rain event. Generally, the duration of rain events showed no significant relationship ($p > 0.05$; linear regression) to average rainfall intensity (the ratio of total rainfall to rain event duration) or total rainfall. Average rain intensity had a well-correlated, significant positive relationship with total rainfall ($r^2 = 0.80$, $p < 0.01$; linear regression), and it is therefore difficult to determine if either one is a more important factor with respect to ^{7}Be wet deposition. An exception to this is the Typhoon Melor event, which was a relatively short and intense storm, and showed relatively low ^{7}Be activity in rainwater (1.3 Bq L^{-1}), and relatively high ^{7}Be wet deposition (174 Bq m^{-2}).

The dry deposition fluxes measured at the UCSC site ($n = 14$) ranged from below detection (typically about 0.01 Bq m^{-2} d^{-1}) to 0.45 Bq m^{-2} d^{-1} (Table 2). Measurements taken during the wet season were generally below detection, but those from the dry season usually had detectable ^{7}Be deposition. This is consistent with the majority of ^{7}Be being removed from the atmosphere via rainfall in the wet season. The average dry season ^{7}Be deposition was 0.2 Bq m^{-2} d^{-1}. Extrapolating this to a monthly basis, the dry deposition was about 7 Bq m^{-2} month^{-1}. This flux is comparable to the average flux of 7.5 Bq m^{-2} month^{-1} observed in the dry months of Mediterranean Spain by Lozano et al. (2011). Nevertheless, one potential confounding factor in the dry deposition measurements is the regular occurrence of fog in the coastal central California area. During the dry summer in Monterey Bay, a shallow cyclonic circulation (the Santa Cruz eddy) occurs on most days (78–79%), causing widespread coastal fog in the Santa Cruz area (Archer et al., 2005). This fog likely impacts the removal rate of ^{7}Be from the atmosphere, and it is unknown whether or not the standard "pot" collector used here is effective in capturing this fog deposition.

Table 2
Beryllium-7 dry deposition samples from coastal sites in northern Monterey Bay. Uncertainties reflect propagated errors arising from 1σ counting error. Location of collection sites UCSC and DSC are shown on Fig. 1.

Site	Time interval (Month/day/year)	^{7}Be (Bq m^{-2})	^{7}Be (Bq m^{-2} d^{-1})
UCSC	03/14/10–03/19/10	2.0 ± 0.5	0.40 ± 0.10
DSC	03/14/10–03/19/10	<0.6	<0.1
UCSC	04/08/10–04/10/10	<0.6	<0.3
UCSC	04/13/10–04/18/10	<0.6	<0.1
UCSC	04/21/10–04/22/10	<0.6	<0.6
UCSC	04/22/10–04/26/10	<0.6	<0.1
UCSC	06/05/10–06/11/10	<0.6	<0.1
UCSC	06/11/10–06/15/10	<0.6	<0.1
UCSC	06/17/10–06/23/10	1.4 ± 0.3	0.23 ± 0.05
UCSC	06/27/10–07/02/10	0.63 ± 0.30	0.13 ± 0.06
UCSC	07/02/10–07/07/10	0.84 ± 0.43	0.17 ± 0.09
UCSC	07/14/10–07/20/10	1.6 ± 0.5	0.27 ± 0.08
UCSC	07/20/10–07/26/10	2.6 ± 0.5	0.45 ± 0.08
UCSC	07/26/10–08/03/10	0.65 ± 0.49	0.08 ± 0.06
UCSC	08/03/10–08/09/10	<0.6	<0.1

3.3. Site differences and temporal trends

To test how representative the site was for rainfall in the Santa Cruz area, rainwater samples were collected simultaneously at the UCSC and DSC sites for a subset of the rainfall events (Table 1). The two sites are about 4 km apart, and differ in elevation by about 230 m (Fig. 1). Rainfall was higher at UCSC relative to the DSC site, with relative percent differences of 21, 46, 63, and 96% between sample pairs. This difference likely reflects the higher elevation of UCSC (250 m) compared to the DSC site (20 m) and the associated orographic effect of the Santa Cruz Mountains. Although there are few ($n = 4$) sample pairs for statistical comparison, a paired t-test for ^{7}Be activity (Bq L^{-1}) in rainwater suggests little difference between the sites ($p = 0.45$). The ^{7}Be wet deposition (Bq m^{-2}) was always higher at UCSC relative to the DSC site, with relative percent differences of 18, 44, 44, and 88% between sample pairs. This difference reflects the higher rainfall at UCSC and the relative similarity of ^{7}Be activity per volume between sites.

The temporal trends of ^{7}Be activity in rainwater and ^{7}Be wet deposition collected at UCSC (Fig. 4) were investigated assuming a monotonous increase or decrease during the rainy season. A simple linear-regression analysis was used to identify overall trends with sampling time as the independent variable and ^{7}Be activity as the dependent variable, with a significant ($p \leq 0.05$) slope indicating a change over time. The regression results show that there was no rainy season trend in ^{7}Be activity in rainwater ($p = 0.78$, Fig. 4A) or in ^{7}Be wet deposition per rain event ($p = 0.074$, Fig. 4B). When considering events with greater than 10 mm rainfall, however,

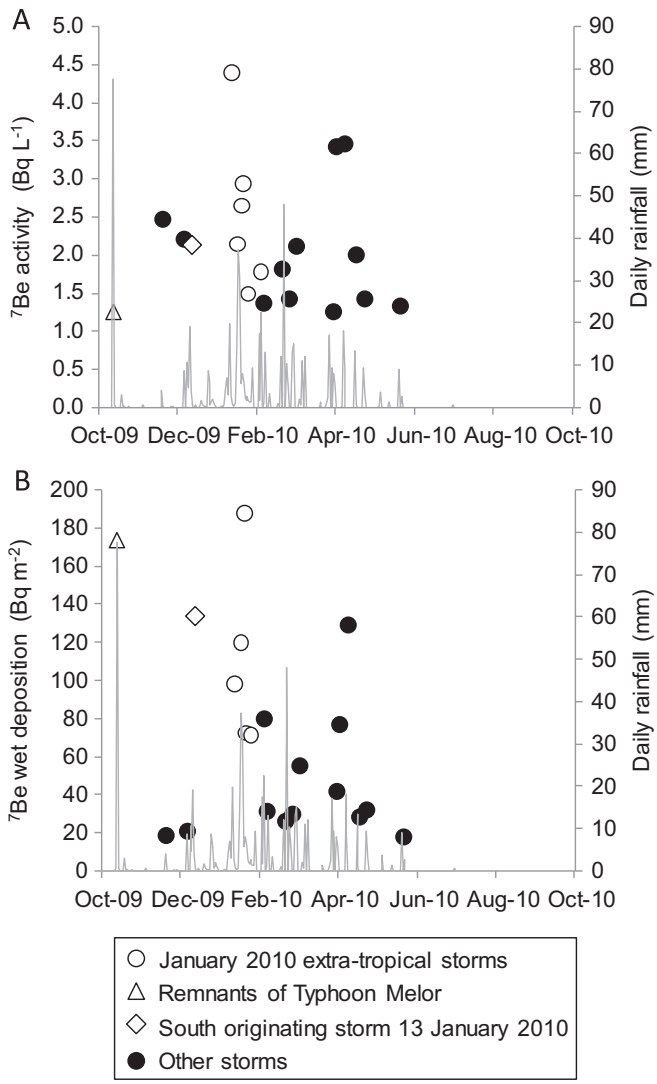

Fig. 4. Time series plots of ^{7}Be activity in rainwater samples taken from the UCSC site. A) ^{7}Be activity in rainfall. B) ^{7}Be wet deposition per rain event. Daily rainfall values are shown as the solid gray line.

there was a significant ($p = 0.003$) decrease in ^{7}Be wet deposition per rain event over the course of the rainy season (Fig. 4B). This reflects that most (60%) of the rainfall in the rainy season occurred between the beginning of December and March.

For many radionuclides that exist in the atmosphere in particulate form, such as ^{7}Be, large rainfall events can wash these particulates out of the atmosphere, causing a decrease in measured radionuclide activity over the course of a prolonged rain event (i.e., a washout effect). The washout effect was investigated by examining four rain samples collected sequentially over a 10-d rainy interval (16–26 January 2010), part of the series of large, extra-tropical storms described above. These samples showed no significant trend in ^{7}Be activity (Bq L^{-1}) or ^{7}Be wet deposition ($p = 0.55$ and 0.41, respectively). This implies that for these storms, the predominant source of ^{7}Be was not local washout and that most of the ^{7}Be was accumulated and transported over a long distance, or that the air mass was constantly replenished with ^{7}Be. The lack of a pronounced washout effect is consistent with observations of Harvey and Matthews (1989), who in a study of a high-rainfall area in New Zealand concluded that the best predictor of ^{7}Be deposition is a simple linear relationship with rainfall amount.

3.4. Annual ^{7}Be deposition

The sampling strategy in this study was designed predominantly to capture deposition from single rain events, and as such the sampling did not span the entire year (leaving out some of the dry season), or sample every day. Nevertheless, based on some assumptions and extrapolations presented here, an annual ^{7}Be flux for the sampling area can be estimated. Atmospheric deposition was sampled on 132 d of the water year (October 2009–September 2010). An actual ^{7}Be deposition of 1450 ± 50 Bq m^{-2} was recorded over this time, with 1440 Bq m^{-2} in intervals with measurable rainfall (45 d) and about 10 Bq m^{-2} as dry deposition (87 d). The sampling captured about 70% of the rainfall by volume for the year, and for purposes of the annualized deposition, it can be assumed that the volume-weighted ^{7}Be activity in the sampling was representative of the other 30% of rainfall, representing another 433 Bq m^{-2}. For dry deposition, most of the unsampled days had no measurable precipitation, with much of this time represented by extended (>5 d) dry intervals, such as the exceptionally dry November 2009 and the late dry season months of August–September 2010. For this estimate, the observed dry season ^{7}Be flux (0.2 Bq m^{-2} d^{-1}) can be applied to the unsampled dry season days ($n = 60$), for another 13 Bq m^{-2}. Taking these estimates for missing wet and dry deposition into account, the pattern of monthly ^{7}Be deposition totals (Fig. 5) are similar to the pattern of monthly rainfall totals, and the estimated annual ^{7}Be flux is 1900 Bq m^{-2} yr^{-1}. This is just below the low end of the range 2000–3800 Bq m^{-2} yr^{-1} (0.033–0.062 dpm cm^{-2} d^{-1}) inferred by Sommerfield et al. (1999) for northern coastal California based on the data from coastal sites for latitudes 30–41°N compiled by Kadko and Olson (1996). The annual flux estimated here is higher than the 834 Bq m^{-2} y^{-1} reported by Lozano et al. (2011) for a coastal site on the Mediterranean coast of Spain, which has a similar latitude (37°N) and climate to coastal California, but within the range 1100–2240 Bq m^{-2} y^{-1} observed by Ródenas et al. (1997) in Cantabria (43°N) on the Atlantic coast of Spain. It must be noted that if it is assumed that dry month measured depositions remain constant through the year (which clearly they do not), dry deposition would account for about 4% of the bulk ^{7}Be fallout. This percentage is somewhat low when compared to values (~10%) observed in other studies at similar latitudes (Olsen et al., 1985;

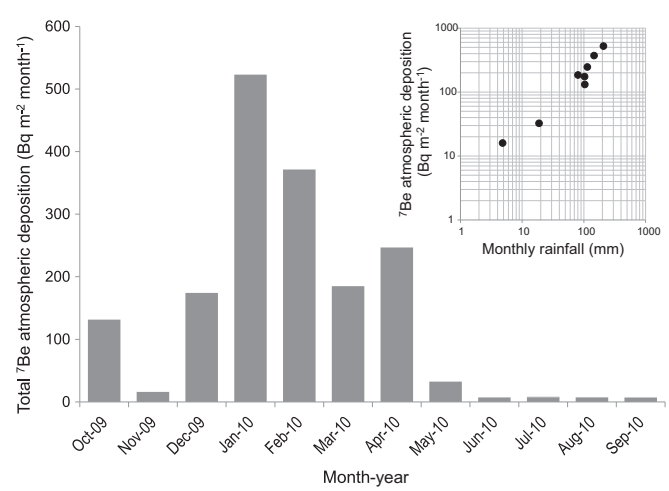

Fig. 5. Estimated monthly ^{7}Be deposition (Bq m^{-2} month^{-1}) in Santa Cruz, CA. The inset in upper right plots the monthly ^{7}Be deposition for wet season months versus monthly rainfall (log–log scale), showing a linear relationship. Total annual ^{7}Be deposition was 1900 Bq m^{-2}.

Todd et al., 1989; Lozano et al., 2011). It is speculated that this difference may be related to the importance of high-precipitation storms originating from the south (Fig. 3) and with enhanced stratospheric–tropospheric exchange and injection of ^{7}Be associated with the relatively large storm events (Typhoon Melor and the record-setting events of January 2010) that occurred in this study.

3.5. San Lorenzo River surface water

Surface-water samples ($n = 23$) collected from the San Lorenzo River during the rainy season covered a variety of storm events and hydrologic conditions (Table 3). There was a wide range of particulate ^{7}Be activity with discharge (Fig. 6), from less than detection (varies with sample geometry, but typically about 0.01 Bq g^{-1}) to 0.6 Bq g^{-1} and an outlier ($p < 0.01$; Grubb's test) at 1.4 Bq g^{-1}. With the outlier value removed, the average activity was 0.29 ± 0.17 Bq g^{-1}, median 0.26 Bq g^{-1}. The range of activity observed was consistent with a typical 0.1–0.2 Bq g^{-1} found for suspended sediment in streams elsewhere (Dominik et al., 1987; Bonniwell et al., 1999; Matisoff et al., 2002; Kaste and Baskaran, 2011).

While examining the temporal and spatial variability of particulate ^{7}Be activity in the San Lorenzo River, we recognize three key controls: the current ^{7}Be inventory in soils and sediment; the intensity of erosion produced by rain events; and the relative contribution of diverse sediment sources, such as surface soil, banks, in-channel sources, and mass wasting. The ^{7}Be inventory in the watershed is a function of inputs from atmospheric deposition, predominantly from antecedent rainfall over the year, export from soil and sediment erosion from storm events, and ^{7}Be loss via radioactive decay (Walling et al., 2009). Prolonged and intense surface runoff would tend to remove the upper layer of ^{7}Be-enriched soil, and entrain deeper soil with less ^{7}Be activity (Wallbrink and Murray, 1996; Blake et al., 1999; Walling et al., 1999; Wilson et al., 2003). As a result, average particulate ^{7}Be activity would tend to be lower for relatively larger storm events. Debris flows can be a result of high-intensity, long-duration rain events (Wieczorek, 1987), and such mass wasting is likely to add much older sediment (with low ^{7}Be activity) to that otherwise being transported in the river. High stream discharge can also cause disruption of armored layers in stream channels and result in the suspension of previously sequestered sediment (Williams, 1989; Bravo-Espinosa et al., 2003), which likely would have very low ^{7}Be activity.

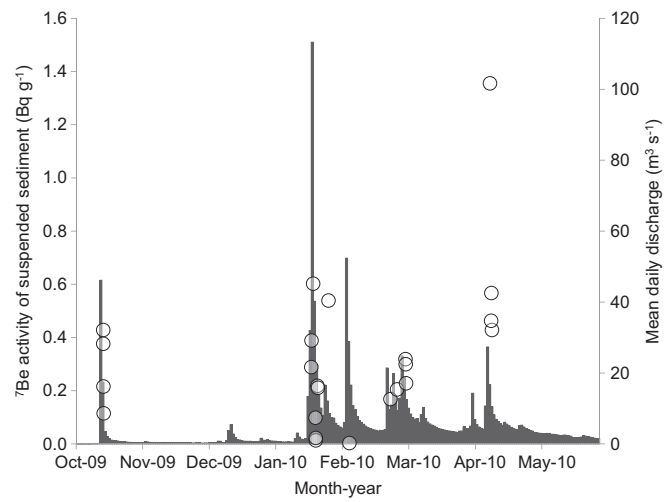

Fig. 6. Time series plot of ^{7}Be activity in suspended sediment (particulate ^{7}Be activity) in San Lorenzo River water samples. The mean daily discharge values for the river are shown as grey shading.

Small, mountainous coastal river systems, such as the San Lorenzo River, are characterized by flashy hydrology and high sediment discharge per unit area (sediment yield) compared to other river systems, and thus this type of watershed contributes disproportionally large sediment and particulate loads to the global ocean (Milliman and Syvitski, 1992; Milliman and Farnsworth, 2011); sediment transport in these systems is predominantly of an episodic nature (Best and Griggs, 1991; Draut et al., 2009; Milliman and Farnsworth, 2011; Conaway et al., 2012). Consequently, erosion and resuspension of relatively older stream or bank sediment may produce a substantial amount of ^{7}Be-depleted sediment.

Table 3
San Lorenzo River surface water, discharge data, suspended sediment concentration (SSC), particulate ^{7}Be activity in surface water, and load calculations for ^{7}Be and suspended sediment. Stream-flow data from the U.S. Geological Survey National Water Information System (NWIS) for gaging station 11161000 (San Lorenzo River at Santa Cruz, CA, http://waterdata.usgs.gov/usa/nwis/uv?11161000).

Collection date (Month/day/year)[a]	Collection time (Hour/minute)[a]	River discharge (m^3 s^{-1})	SSC (mg L^{-1})	Particulate ^{7}Be (Bq g^{-1})	^{7}Be load (Bq s^{-1})	Suspended sediment load (kg s^{-1})
10/13/09	14:00	37	335	0.40	5258	12
10/13/09	17:00	94	637	0.22	12,960	60
10/13/09	19:00	125	685	0.12	9811	85
01/18/10	12:45	8	239	0.29	579	2
01/18/10	16:15	42	386	0.39	6245	16
01/19/10	10:00	17	88	0.60	878	1
01/20/10	11:45	308	1615	0.10	49,230	498
01/20/10	15:49	225	2834	0.01	8520	638
01/20/10	15:55	210	2614	0.02	12,299	548
01/21/10	10:30	37	150	0.22	1224	6
01/21/10	14:30	40	114	0.21	950	4
01/26/10	13:30	21	103	0.54	1146	2
02/05/10	08:30	62	420	<0.01	<260	26
02/24/10	10:30	35	211	0.17	1229	7
02/27/10	12:25	21	54	0.21	227	1
03/03/10	10:51	20	109	0.32	711	2
03/03/10	13:10	38	192	0.30	2196	7
03/03/10	17:15	34	161	0.23	1240	5
04/11/10	19:50	25	134	1.4	4629	3
04/12/10	17:30	26	110	0.43	1243	3
04/12/10	11:30	25	90	0.57	1288	2
04/12/10	09:00	25	62	0.46	735	2

[a] All times are given in the local Pacific Time.

An examination of the relationship between suspended sediment load and ^{7}Be load (Fig. 7) apparently shows this effect. There was a strong, significant linear correlation ($r^2 = 0.50$; $p < 0.01$, linear regression) between particulate ^{7}Be activity and $\log_{10}$ transformed suspended sediment concentration (Fig. 7A), and this relationship provided the rationale to create a model to predict ^{7}Be load based on suspended sediment load (Fig. 7B). The high end of the linear trend in Fig. 7B represents the peak discharge of the large January 2010 storm event, when the greatest sediment erosion presumably occurred. The high-load values for the falling limb of the January flood peak had high standard residuals (≥2) in preliminary regression modeling, suggesting that they can be treated as outliers from the rest of the data. Although there are few data to compare, the sample collected on the rising limb of the January flood peak had a 5-fold higher ^{7}Be load ($10^{4.7}$ Bq s^{-1}) than the samples collected on the falling limb (about $10^{4.0}$ Bq s^{-1}). As described in Conaway et al. (2012), this particular flood event was characterized by a shift to greater suspended-sediment concentration per unit discharge on the falling limb of the flood, i.e., reverse hysteresis. The hysteresis shows simultaneous peaks of discharge and suspended-sediment concentration, but a factor of 1.7 higher sediment load on the falling limb than the rising limb for equivalent discharge values. This difference in sediment load was attributed to high soil erodibility, in conjunction with prolonged erosion during flooding (Conaway et al., 2012); the ^{7}Be load data support this explanation, suggesting that a substantial amount of ^{7}Be-depleted soil was mobilized. We note that although ^{7}Be adsorption commonly shows a dependence on sediment grain size (Kaste and Baskaran, 2011), there was only a small range of variation in grain size observed in surface water samples taken from the river over the course of the storm event (Draut et al., 2011).

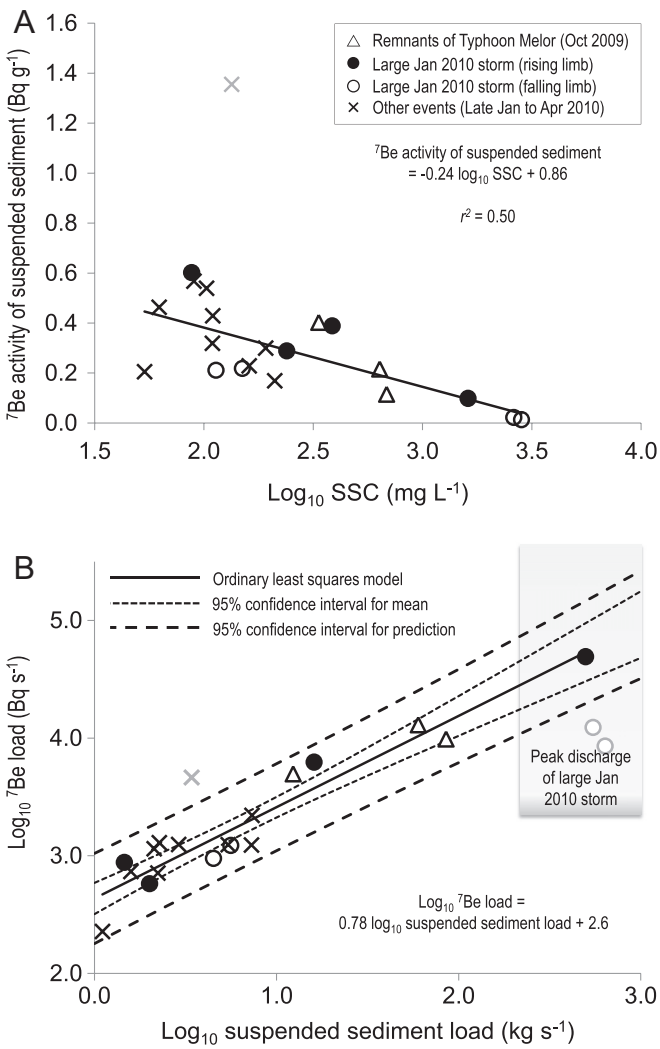

Fig. 7. Statistical examination of particulate ^{7}Be activity and load to suspended sediment concentrations and load in the San Lorenzo River. Data from large rain events are illustrated with unique markers, including the remnants of Typhoon Melor and both the rising and falling parts of the hydrograph for the large January 2010 storm event. Other storm event data (January to April 2010) are not subdivided. A) Linear regression analysis showing statistically significant strong correlation of particulate ^{7}Be activity and $\log_{10}$ transformed suspended sediment concentration ($r^2 = 0.50$; $p < 0.01$). One outlier (marker shown in grey) was excluded from the analysis. B) Least squares model to predict ^{7}Be load based on suspended sediment concentration. The area of peak stream discharge and suspended sediment transport for the January 2010 storm (the largest event of the year) is highlighted with grey. Data were $\log_{10}$ transformed to improve normality for the ordinary least squares model. Values with high standardized residuals (markers shown in grey), were excluded from the final model output.

3.6. Storm event ^{7}Be load and watershed retention

The large flood in the San Lorenzo River on 17–23 January 2010 mobilized about 65% of the annual sediment load for the watershed (Conaway et al., 2012). Beryllium-7 particulate activities near peak discharge were lower on the falling limb of the flood than on the rising limb, but returned to typical values (0.2 Bq g^{-1}) near the end of the storm event. A surface water sample collected in the next major flood event on 5 February 2010 had no detectable ^{7}Be (<0.01 Bq g^{-1}), suggesting that the sediment in the river at that time was dominated by ^{7}Be-depleted material. The subsequent series of relatively smaller flood events in late February to early March 2010 had more typical particulate ^{7}Be values (0.17–0.32 Bq g^{-1}). These changes are inferred to reflect changes in sediment sources and erosion over the course of a few flood events, as well as the retention of ^{7}Be in the San Lorenzo River watershed, similar to observations from other systems (Dominik et al., 1987; Cooper et al., 1991; Bonniwell et al., 1999; Kaste and Baskaran, 2011). Moreover, these changes suggest that if using a ^{7}Be inventory-based approach to assess the contribution of fluvial sediment in local nearshore marine deposits (e.g., Sommerfield et al., 1999; Corbett et al., 2007; Jweda et al., 2008; Draut et al., 2009), it would be difficult to discriminate between relatively older or newer pulses of recent (<1 yr) flood sedimentation from the San Lorenzo River deposited in Monterey Bay.

To further investigate the retention of atmospherically derived ^{7}Be in the watershed, it would be useful to compare rainfall and ^{7}Be atmospheric deposition with discharge and ^{7}Be load in the river during the large January 2010 storm. Unfortunately, there were too few particulate ^{7}Be data to generate a model for a quantitative comparison. The difficulties in determining a ^{7}Be load are that: a) the majority of the sediment for the event is transported in the falling limb of the hydrograph (about 1.7 × higher suspended-sediment concentration for a given discharge in falling versus rising); b) there are too few ^{7}Be data near the flood peak or in the falling limb; c) the falling limb lies off the linear trend shown in Fig. 7B; and d) available ^{7}Be values for the falling limb are about 5-fold less than those observed during the rising limb. The result is that a linear ^{7}Be-load/suspended sediment-load model will overpredict ^{7}Be loads unless they are heavily biased toward the ^{7}Be-depleted values near peak discharge. To briefly illustrate this, using the ordinary least squares model in Fig. 7B and the suspended sediment concentration (SSC) data from Conaway et al. (2012), the ^{7}Be load for 16–24 January 2010 is calculated to be 7×10^{11} Bq, which is 7-fold higher than the ^{7}Be deposition during the rain event (about 380 Bq m^{-2}, or about 1.1×10^{11} Bq over the watershed area), and somewhat higher

than even the annual atmospheric deposition to the watershed ($\sim 5.7 \times 10^{11}$ Bq), clearly an impossible situation.

It is worth noting, however, that the linear model in Fig. 7B appears to work well considering only data from before when the suspended-sediment concentration–discharge relationship began to shift. If a conservative approach is taken, using only the ^{7}Be transported during the rising limb of the hydrograph where all data appear to be fit well, the ^{7}Be load is 8.4×10^{10}, which is about 73% of the estimated atmospheric deposition over the rain event, or about 46% of all of the decay-corrected ^{7}Be wet deposition from October 2009 up until and including the rain event. Nevertheless, even allowing for the 95% confidence interval in the model (which gives a range of 25–200% watershed export), this conservative estimate is far higher than observed watershed yields of ^{7}Be observed elsewhere, which are typically less than 10% (Dominik et al., 1987; Cooper et al., 1991). These results may suggest greater export of ^{7}Be from small mountainous river systems, with their characteristic flashy hydrology and high sediment yield, but the ^{7}Be load model's resolution is poor and further detailed studies with higher-resolution sampling near peak sediment discharge would be required to refine these relations.

4. Summary

This paper presents the first ^{7}Be atmospheric deposition data for the central California coast, examines individual events and short-term seasonal variability of ^{7}Be in rain events, and investigates ^{7}Be in corresponding flood events in a Pacific coastal watershed. The temporal and spatial variability of ^{7}Be accumulation quantified here comprise one of few such data sets for this commonly used geochemical tracer, and as such could better define its uses and limitations for future studies. Generally, the observed ^{7}Be activities in rainwater and ^{7}Be deposition were comparable to those observed at other coastal locations with similar latitude and climate, such as Mediterranean Spain. Beryllium-7 wet deposition appeared to decrease over the course of the rainy season and ^{7}Be wet deposition was largely a function of total rainfall for a given rain event regardless of the storm arrival direction. The surface water ^{7}Be particulate activities showed that small, mountainous river systems, with their high sediment yields compared to other watersheds, may have a linear relationship between ^{7}Be load and sediment load at low to moderate wet-season storm events, but can mobilize substantial ^{7}Be-depleted sediment in larger events, such as the 5-y flood event that occurred in the study area during January 2010. These findings illustrate the behavior of ^{7}Be atmospheric deposition and potential utility of ^{7}Be in investigating sediment transport processes in a small, mountainous river watershed in a Mediterranean climate, but also possible pitfalls of using this tracer to identify individual flood pulses of sediment deposited in the coastal ocean.

Acknowledgments

Funding was provided by the USGS Mendenhall Postdoctoral Research Fellowship to C.H. Conaway. ICP-MS measurements were performed at the UCSC Institute of Marine Sciences Marine Analytical Laboratory with the assistance of Rob Franks. Preparation of acid-cleaned equipment and wet chemistry procedures were performed in Professor A.R. Flegal's laboratory at UCSC. Access to the UCSC rooftop was provided by Jim Velzy. Sampling and other analytical assistance was provided by Kingsley Odigie, Leticia Diaz, Peter Weiss-Penzias, Daryl McGinnis, and Ken Bencala. San Lorenzo River sampling assistance was provided by personnel from the U.S. Geological Survey's Pacific Coastal and Marine Science Center, including Jackson Currie, Peter Harkins, Cordell Johnson, and Andy Ritchie. Comments on the manuscript were graciously provided by M. Baskaran, C.C. Fuller, Christopher G. Smith, Shun-ichi Hisamatsu, and two anonymous reviewers. Any use of trade names is for descriptive purposes only and does not imply endorsement by the U.S. Government.

References

Archer, C.L., Jacobson, M.Z., Ludwig, F.L., 2005. The Santa Cruz eddy. Part I: observations and statistics. Monthly Weather Rev. 133, 767–782.
Arnold, J.R., Al-Salih, H.A., 1955. Beryllium-7 produced by cosmic rays. Science 121, 451–453.
Ayub, J.J., Di Gregorio, D.E., Velasco, H., Huck, H., Rizzotto, M., Lohaiza, F., 2009. Short-term seasonal variability in Be-7 wet deposition in a semiarid ecosystem of central Argentina. J. Environ. Radioact. 100, 977–981.
Baskaran, M., 1995. A search for the seasonal variability on the depositional fluxes of ^{7}Be and ^{210}Pb. J. Geophys. Res. -Atmos. 100, 2833–2840.
Baskaran, M., Coleman, C.H., Santschi, P.H., 1993. Atmospheric depositional fluxes of ^{7}Be and ^{210}Pb at Galveston and College Station, Texas. J. Geophys. Res.-Atmos. 98, 20555–20571.
Baskaran, M., Swarzenski, P.W., 2007. Seasonal variations on the residence times and partitioning of short-lived radionuclides (^{234}Th, ^{7}Be and ^{210}Pb) and depositional fluxes of ^{7}Be and ^{210}Pb in Tampa Bay, Florida. Mar. Chem. 104, 27–42.
Berggren, A.M., Beer, J., Possnert, G., Aldahan, A., Kubik, P., Christl, M., Johnsen, S.J., Abreu, J., Vinther, B.M., 2009. A 600-year annual ^{10}Be record from the NGRIP ice core, Greenland. Geophys. Res. Lett. 36
Best, T.C., Griggs, G.B., 1991. A sediment budget for the Santa Cruz litoral cell, California. In: SEPM (Ed.), From Shoreline to Abyss. Society for Sedimentary Geology, pp. 35–50. SEPM Special Publication No. 46.
Blake, W.H., Walling, D.E., He, Q., 1999. Fallout beryllium-7 as a tracer in soil erosion investigations. Appl. Radiat. Isot. 51, 599–605.
Bonniwell, E.C., Matisoff, G., Whiting, P.J., 1999. Determining the times and distances of particle transit in a mountain stream using fallout radionuclides. Geomorphology 27, 75–92.
Bravo-Espinosa, M., Osterkamp, W.R., Lopes, V.L., 2003. Bedload transport in alluvial channels. J. Hydraulic Eng. 129, 783–795.
Caillet, S., Arpagaus, P., Monna, F., Dominik, J., 2001. Factors controlling ^{7}Be and ^{210}Pb atmospheric deposition as revealed by sampling individual rain events in the region of Geneva, Switzerland. J. Environ. Radioact. 53, 241–256.
Conaway, C.H., Draut, A.E., Echols, K.R., Storlazzi, C.D., Ritchie, A., 2012. Episodic suspended sediment transport and elevated polycyclic aromatic hydrocarbon concentrations in a small, mountainous river in coastal California. River Res. Appl.. http://dx.doi.org/10.1002/rra.2582
Cooper, L.W., Olsen, C.R., Solomon, D.K., Larsen, I.L., Cook, R.B., Grebmeier, J.M., 1991. Stable isotopes of oxygen and natural and fallout radionuclides used for tracing runoff during snowmelt in an Arctic watershed. Water Resour. Res. 27, 2171–2179.
Corbett, D.R., Dail, M., McKee, B., 2007. High-frequency time-series of the dynamic sedimentation processes on the western shelf of the Mississippi River Delta. Cont. Shelf Res. 27, 1600–1615.
Dominik, J., Burrus, D., Vernet, J.P., 1987. Transport of the environmental radionuclides in an alpine watershed. Earth Planetary Sci. Lett. 84, 165–180.
Draut, A.E., Bothner, M.H., Field, M.E., Reynolds, R.L., Cochran, S.A., Logan, J.B., Storlazzi, C.D., Berg, C.J., 2009. Supply and dispersal of flood sediment from a steep, tropical watershed: Hanalei Bay, Kaua'i, Hawai'i, USA. Geol. Soc. Am. Bull. 121, 574–585.
Draut, A.E., Conaway, C.H., Echols, K.R., Storlazzi, C.D., Ritchie, A., 2011. Suspended Sediment and Organic Contaminants in the San Lorenzo River, California, Water Years 2009–2010: U.S. Geological Survey Open-file Report 2011-1120, p. 24.
Draxler, R.R., Rolph, G.D., 2012. HYSPLIT (HYbrid Single-particle Lagrangian Integrated Trajectory) Model Access via NOAA ARL READY. NOAA Air Resources Laboratory, Silver Spring, MD. Website: http://ready.arl.noaa.gov/HYSPLIT.php.
Farnsworth, K.L., Milliman, J.D., 2003. Effects of climatic and anthropogenic change on small mountainous rivers: the Salinas River example. Glob. Planet. Change 39, 53–64.
Graham, I., Ditchburn, R., Barry, B., 2003. Atmospheric deposition of ^{7}Be and ^{10}Be in New Zealand rain (1996–98). Geochim. Cosmochim. Acta 67, 361–373.
Harvey, M.J., Matthews, K.M., 1989. ^{7}Be deposition in a high-rainfall area of New Zealand. J. Atmos. Chem. 8, 299–306.
Hawley, N., Robbins, J.A., Eadie, B.J., 1986. The partitioning of ^{7}beryllium in fresh water. Geochim Cosmochim Acta 50, 1127–1131.
Husain, L., Coffey, P.E., Meyers, R.E., Cederwall, R.T., 1977. Ozone transport from stratosphere to troposphere. Geophys. Res. Lett. 4, 363–365.
Inman, D.L., Jenkins, S.A., 1999. Climate change and the episodicity of sediment flux of small California rivers. J. Geol. 107, 251–270.
Ishikawa, Y., Murakami, H., Sekine, T., Yoshihara, K., 1995. Precipitation scavenging studies of radionuclides in air using cosmogenic ^{7}Be. J. Environ. Radioact. 26, 19–36.
Jweda, J., Baskaran, M., van Hees, E., Schweitzer, L., 2008. Short-lived radionuclides (Be-7 and Pb-210) as tracers of particle dynamics in a river system in southeast Michigan. Limnol. Oceanogr. 53, 1934–1944.
Kadko, D., Olson, D., 1996. Beryllium-7 as a tracer of surface water subduction and mixed-layer history. Deep-Sea Res. Part I 43, 89–116.

Kaste, J.M., Baskaran, M., 2011. Meteoric ^{7}Be and ^{10}Be as process tracers in the environment. In: Baskaran, M. (Ed.), Handbook of Environmental Isotope Geochemistry. Springer-Verlag, Berlin.

Koch, D.M., Jacob, D.J., Graustein, W.C., 1996. Vertical transport of tropospheric aerosols as indicated by Be-7 and Pb-210 in a chemical tracer model. J. Geophys. Res.-Atmos. 101, 18651–18666.

Lozano, R.L., San Miguel, E.G., Bolívar, J.P., Baskaran, M., 2011. Depositional fluxes and concentrations of ^{7}Be and ^{210}Pb in bulk precipitation and aerosols at the interface of Atlantic and Mediterranean coasts in Spain. J. Geophys. Res. -Atmos. 116, D18213.

Masarik, J., Beer, J., 2009. An updated simulation of particle fluxes and cosmogenic nuclide production in the Earth's atmosphere. J. Geophys. Res.-Atmos. 114

Matisoff, G., Bonniwell, E.C., Whiting, P.J., 2002. Soil erosion and sediment sources in an Ohio watershed using beryllium-7, cesium-137, and lead-210. J. Environ. Qual. 31, 54–61.

Matisoff, G., Wilson, C.G., Whiting, P.J., 2005. The ^{7}Be/^{210}Pb$_{xs}$ ratio as an indicator of suspended sediment age or fraction new sediment in suspension. Earth Surf. Process. Landf. 30, 1191–1201.

Milliman, J.D., Farnsworth, K.L., 2011. River Discharge to the Coastal Ocean: A Global Synthesis. Cambridge University Press, Cambridge.

Milliman, J.D., Syvitski, J.P.M., 1992. Geomorphic tectonic control of sediment discharge to the ocean: the importance of small mountainous rivers. J. Geol. 100, 525–544.

NOAA, 2009. State of the Climate: National Overview for October 2009. National Climatic Data Center. published online November 2009, retrieved on February 22, 2012 from: http://www.ncdc.noaa.gov/sotc/2009/10.

NOAA, 2010. State of the Climate: National Overview for January 2010. National Climatic Data Center. published online February 2010, retrieved on February 16, 2012 from: http://www.ncdc.noaa.gov/sotc/2010/1.

Nuss, W., 1996. National Oceanic and Atmospheric Administration Climate and Meteorology. Last accessed April 14.

NWIS, 2012. U.S. Geological Survey National Water Information System: Web Interface. http://waterdata.usgs.gov/usa/nwis/uv?11161000. Last accessed October 16, 2012.

Olsen, C.R., Larsen, I.L., Lowry, P.D., Cutshall, N.H., Nichols, M.M., 1986. Geochemistry and deposition of ^{7}Be in river-estuarine and coastal waters. J. Geophys. Res.-Oceans 91, 896–908.

Olsen, C.R., Larsen, I.L., Lowry, P.D., Cutshall, N.H., Todd, J.F., Wong, G.T.F., Casey, W.H., 1985. Atmospheric fluxes and marsh soil inventories of ^{7}Be and ^{210}Pb. J. Geophys. Res.-Atmos. 90, 10487–10495.

Pham, M.K., Betti, M., Nies, H., Povinec, P.P., 2011. Temporal changes of ^{7}Be, ^{137}Cs and ^{210}Pb activity concentrations in surface air at Monaco and their correlation with meteorological parameters. J. Environ. Radioact. 102, 1045–1054.

Ródenas, C., Gómez, J., Quindós, L.S., Fernández, P.L., Soto, J., 1997. ^{7}Be concentrations in air, rain water and soil in Cantabria (Spain). Appl. Radiat. Isot. 48, 545–548.

Rolph, G.D., 2012. Real-time Environmental Applications and Display SYstem (READY). NOAA Air Resources Laboratory, Silver Spring, MD. Website: http://ready.arl.noaa.gov.

Sommerfield, C.K., Nittrouer, C.A., Alexander, C.R., 1999. ^{7}Be as a tracer of flood sedimentation on the northern California continental margin. Cont. Shelf Res. 19, 335–361.

Todd, J.F., Wong, G.T.F., Olsen, C.R., Larsen, I.L., 1989. Atmospheric depositional characteristics of beryllium 7 and lead 210 along the southeastern Virginia coast. J. Geophys. Res. -Atmos. 94, 11106–11116.

Turekian, K.K., Benninger, L.K., Dion, E.P., 1983. ^{7}Be and ^{210}Pb total deposition fluxes at New Haven, Connecticut and at Bermuda. J. Geophys. Res.-Oceans Atmos. 88, 5411–5415.

Vonmoos, M., Beer, J., Muscheler, R., 2006. Large variations in Holocene solar activity: constraints from ^{10}Be in the Greenland ice core project ice core. J. Geophys. Res.-Space Phys. 111

Wallbrink, P.J., Murray, A.S., 1994. Fallout of ^{7}Be in south eastern Australia. J. Environ. Radioact. 25, 213–228.

Wallbrink, P.J., Murray, A.S., 1996. Distribution and variability of ^{7}Be in soils under different surface cover conditions and its potential for describing soil redistribution processes. Water Resour. Res. 32, 467.

Walling, D.E., He, Q., Blake, W., 1999. Use of ^{7}Be and ^{137}Cs measurements to document short- and medium-term rates of water-induced soil erosion on agricultural land. Water Resour. Res. 35, 3865–3874.

Walling, D.E., Schuller, P., Zhang, Y., Iroume, A., 2009. Extending the timescale for using beryllium 7 measurements to document soil redistribution by erosion. Water Resour. Res. 45

Whiting, P.J., Matisoff, G., Fornes, W., 2005. Suspended sediment sources and transport distances in the Yellowstone River basin. Geol. Soc. Am. Bull. 117, 515–529.

Wieczorek, G.F., 1987. Effect of rainfall intensity and duration on debris flows in central Santa Cruz Mountains, California. In: Costa, J.E., Wieczorek, G.F. (Eds.), Debris Flows/avalanches – process, Recognition, and Mitigation. Reviews in Engineering Geology, vol. VIII. Geological Society of America, Boulder, Colorado, pp. 93–104.

Williams, G.P., 1989. Sediment concentration versus water discharge during single hydrologic events in rivers. J. Hydrology 111, 89–106.

Wilson, C.G., Matisoff, G., Whiting, P.J., 2003. Short-term erosion rates from a ^{7}Be inventory balance. Earth Surf. Process. Landf. 28, 967–977.

WRCC, 2012. Western Regional Climate Center Western U.S. Climate Historical Summaries, Period of Record Monthly Climate Summary for Santa Cruz, California (047916). retrieved on March 16, 2012 from: http://www.wrcc.dri.edu/cgi-bin/cliMAIN.pl?ca7916. Last accessed.

Yoshimori, M., 2005. Production and behavior of beryllium-7 radionuclide in the upper atmosphere. In: Burrows, J.P., Eichmann, K.U. (Eds.), Atmospheric Remote Sensing: Earth's Surface, Troposphere, Stratosphere and Mesosphere – I. Elsevier Science Ltd, Oxford, pp. 922–926.

You, C.F., Lee, T., Li, Y.H., 1989. The partition of Be between soil and water. Chem. Geol. 77, 105–118.

Zhu, J., Olsen, C.R., 2009. Beryllium-7 atmospheric deposition and sediment inventories in the Neponset River estuary, Massachusetts, USA. J. Environ. Radioact. 100, 192–197.